

1 Supplemental figures to Jacobs et al.

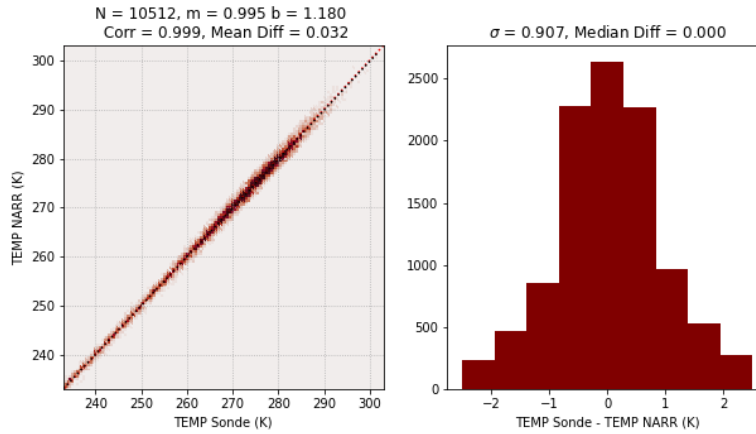


Figure 1: **a)** Scatter plot of the meteorological winter NARR temperature values for NRMN vs the OUN sounding temperature binned to 0.5 K^{-1} . Black line is the least-squares regression, and the red dotted line is the 1-to-1 line. The title displays the slope (m), the intercept (b), the number of points (N), the Pearson correlation (Corr), and the mean difference (Mean Diff). **(b)** The two-dimensional histogram displays the differences in temperature between the sounding data and the NARR data for meteorological winter. The title displays the standard deviation (σ) and the median difference (Median Diff).

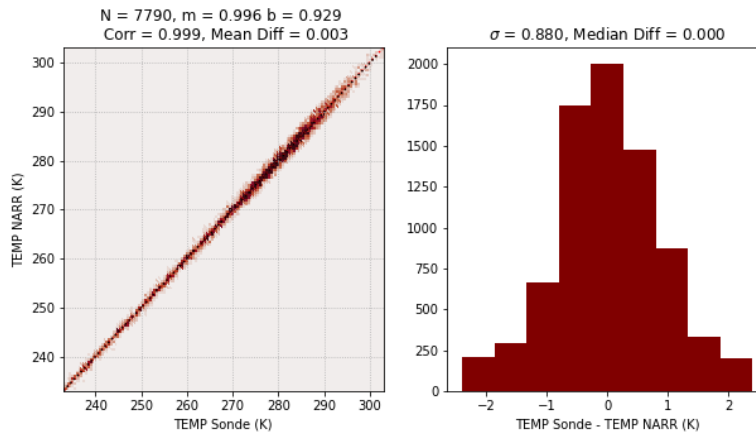


Figure 2: **a)** Scatter plot of the meteorological spring NARR temperature values for NRMN vs the OUN sounding temperature binned to 0.5 K^{-1} . Black line is the least-squares regression, and the red dotted line is the 1-to-1 line. The title displays the slope (m), the intercept (b), the number of points (N), the Pearson correlation (Corr), and the mean difference (Mean Diff). **(b)** The two-dimensional histogram displays the differences in temperature between the sounding data and the NARR data for meteorological spring. The title displays the standard deviation (σ) and the median difference (Median Diff).

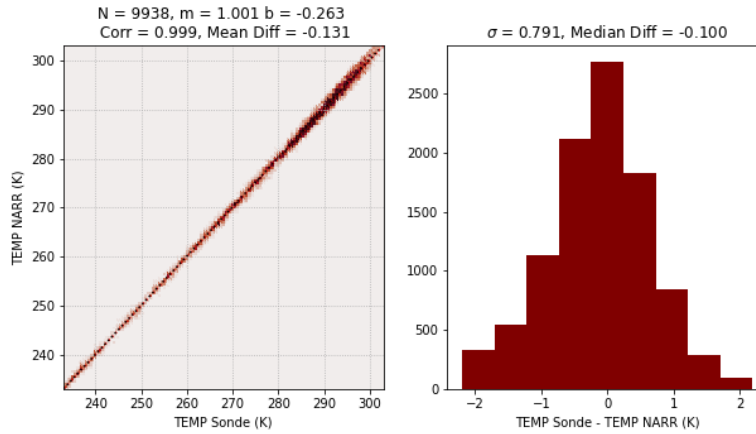


Figure 3: **a)** Scatter plot of the meteorological summer NARR temperature values for NRMN vs the OUN sounding temperature binned to 0.5 K^{-1} . Black line is the least-squares regression, and the red dotted line is the 1-to-1 line. The title displays the slope (m), the intercept (b), the number of points (N), the Pearson correlation (Corr), and the mean difference (Mean Diff). **b)** The two-dimensional histogram displays the differences in temperature between the sounding data and the NARR data for meteorological summer. The title displays the standard deviation (σ) and the median difference (Median Diff).

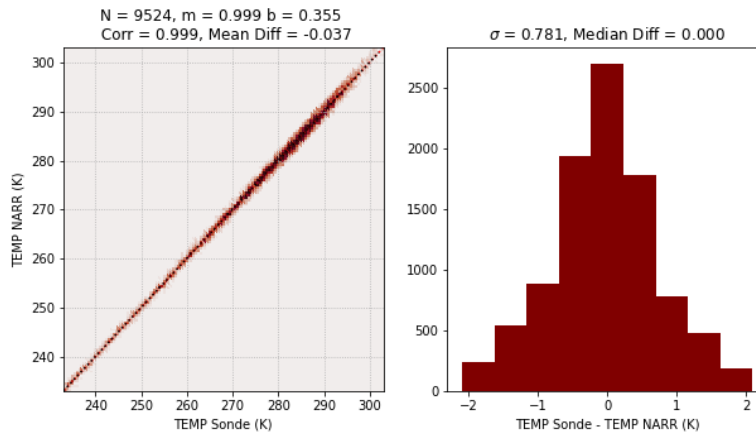


Figure 4: **a)** Scatter plot of the meteorological autumn NARR temperature values for NRMN vs the OUN sounding temperature binned to 0.5 K^{-1} . Black line is the least-squares regression, and the red dotted line is the 1-to-1 line. The title displays the slope (m), the intercept (b), the number of points (N), the Pearson correlation (Corr), and the mean difference (Mean Diff). **(b)** The two-dimensional histogram displays the differences in temperature between the sounding data and the NARR data for meteorological autumn. The title displays the standard deviation (σ) and the median difference (Median Diff).

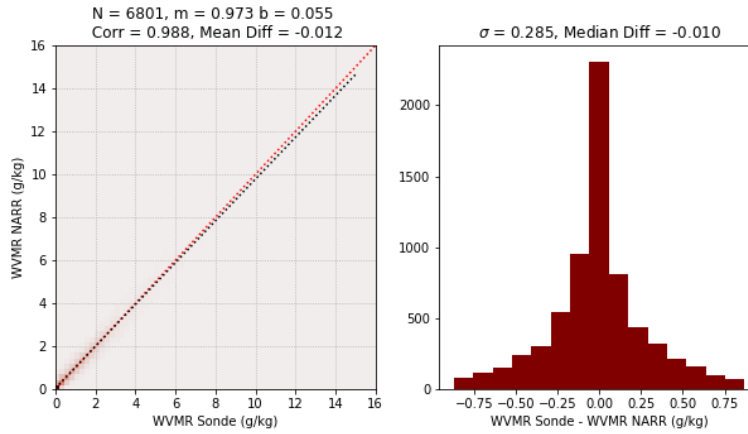


Figure 5: **a)** Scatter plot of the meteorological winter NARR water vapor mixing ratio values for NRMN vs the OUN sounding water vapor mixing ratio binned to 0.25 g/kg^{-1} . Black line is the least-squares regression, and the red dotted line is the 1-to-1 line. The title displays the slope (m), the intercept (b), the number of points (N), the Pearson correlation (Corr), and the mean difference (Mean Diff). **(b)** The two-dimensional histogram displays the differences in water vapor mixing ratio between the sounding data and the NARR data for meteorological winter. The title displays the standard deviation (σ) and the median difference (Median Diff).

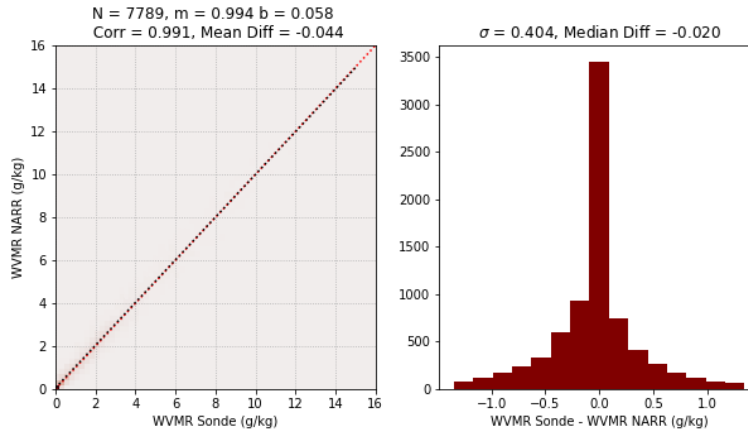


Figure 6: **a)** Scatter plot of the meteorological spring NARR water vapor mixing ratio values for NRMN vs the OUN sounding water vapor mixing ratio binned to 0.25 g/kg^{-1} . Black line is the least-squares regression, and the red dotted line is the 1-to-1 line. The title displays the slope (m), the intercept (b), the number of points (N), the Pearson correlation (Corr), and the mean difference (Mean Diff). **(b)** The two-dimensional histogram displays the differences in water vapor mixing ratio between the sounding data and the NARR data for meteorological spring. The title displays the standard deviation (σ) and the median difference (Median Diff).

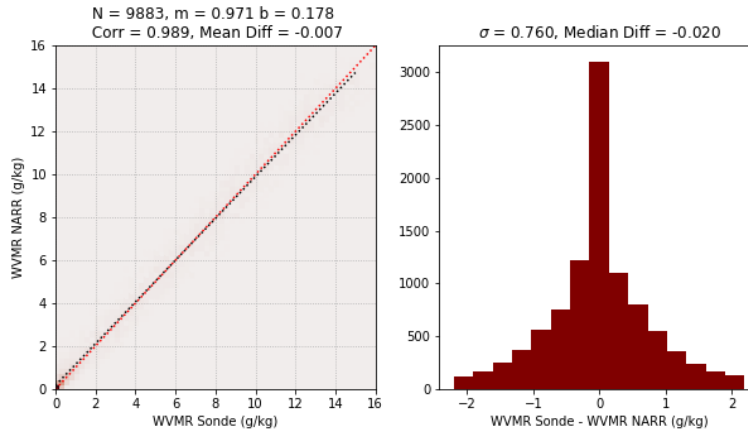


Figure 7: **a)** Scatter plot of the meteorological summer NARR water vapor mixing ratio values for NRMN vs the OUN sounding water vapor mixing ratio binned to 0.25 g/kg^{-1} . Black line is the least-squares regression, and the red dotted line is the 1-to-1 line. The title displays the slope (m), the intercept (b), the number of points (N), the Pearson correlation (Corr), and the mean difference (Mean Diff). **(b)** The two-dimensional histogram displays the differences in water vapor mixing ratio between the sounding data and the NARR data for meteorological summer. The title displays the standard deviation (σ) and the median difference (Median Diff).

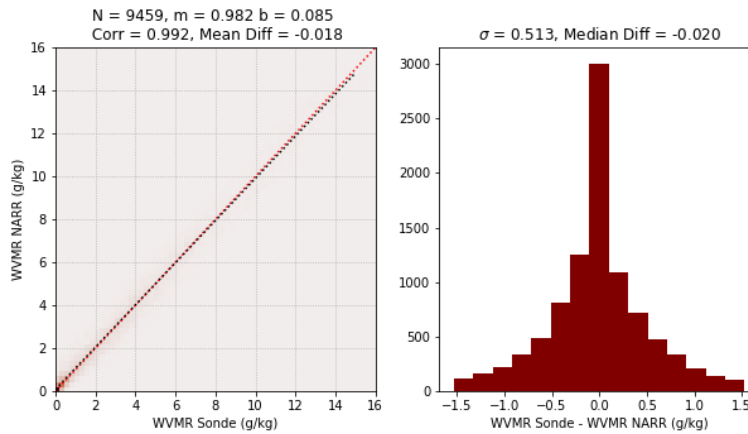


Figure 8: **a)** Scatter plot of the meteorological autumn NARR water vapor mixing ratio values for NRMN vs the OUN sounding water vapor mixing ratio binned to 0.25 g/kg^{-1} . Black line is the least-squares regression, and the red dotted line is the 1-to-1 line. The title displays the slope (m), the intercept (b), the number of points (N), the Pearson correlation (Corr), and the mean difference (Mean Diff). **b)** The two-dimensional histogram displays the differences in water vapor mixing ratio between the sounding data and the NARR data for meteorological autumn. The title displays the standard deviation (σ) and the median difference (Median Diff).

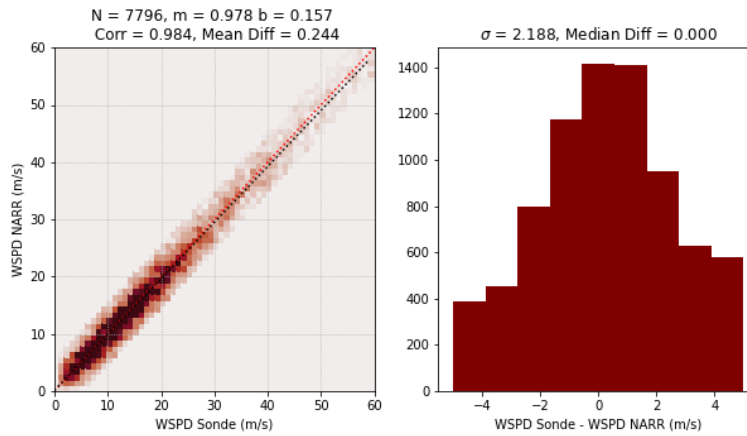


Figure 9: **(a)** Scatter plot of the meteorological spring NARR wind speed values for NRMN vs the OUN sounding wind speed values binned to 1 m s^{-1} . Black line is the least-squares regression, and the red dotted line is the 1-to-1 line. The title displays the slope (m), the intercept (b), the number of points (N), the Pearson correlation (Corr), and the mean difference (Mean Diff). **(b)** The two-dimensional histogram displays the differences in wind speeds between the sounding data and the NARR data for meteorological spring. The title displays the standard deviation (σ) and the median difference (Median Diff).

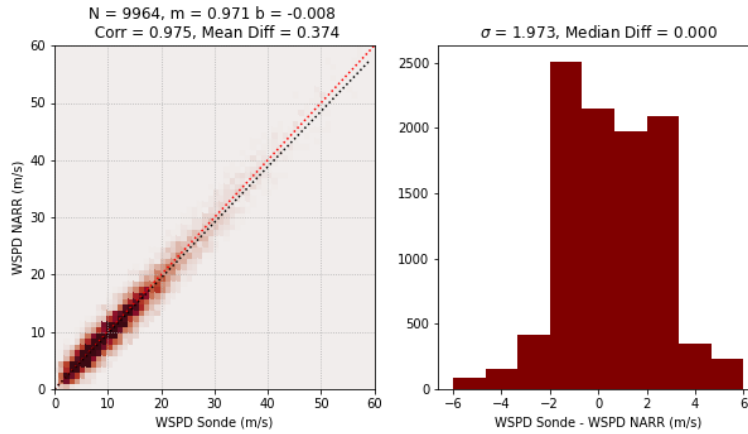


Figure 10: **(a)** Scatter plot of the meteorological autumn NARR wind speed values for NRMN vs the OUN sounding wind speed values binned to 1 m s^{-1} . Black line is the least-squares regression, and the red dotted line is the 1-to-1 line. The title displays the slope (m), the intercept (b), the number of points (N), the Pearson correlation (Corr), and the mean difference (Mean Diff). **(b)** The two-dimensional histogram displays the differences in wind speeds between the sounding data and the NARR data for meteorological autumn. The title displays the standard deviation (σ) and the median difference (Median Diff).

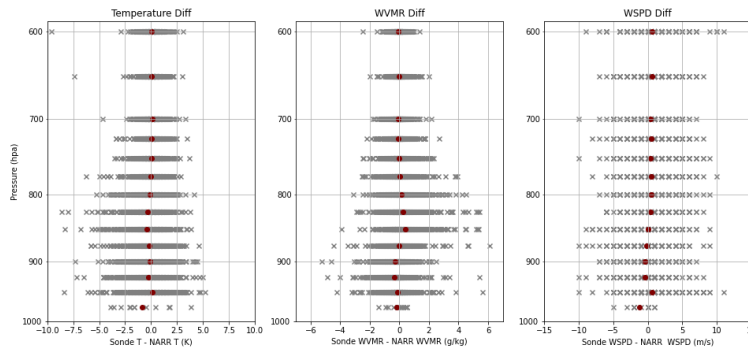


Figure 11: The differences in temperature **(a)**, water vapor mixing ratio **(b)**, and wind speed **(c)** for meteorological spring. Each x marks a difference, with the red symbol representing the mean. Differences are plotted with respect to atmospheric pressure on a logarithmic scale.

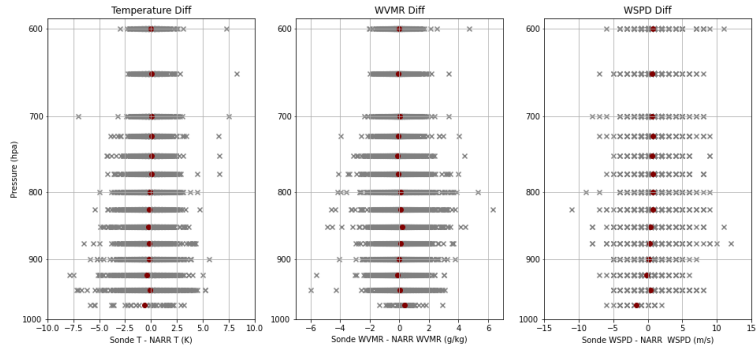


Figure 12: The differences in temperature (a), water vapor mixing ratio (b), and wind speed (c) for meteorological autumn. Each x marks a difference, with the red symbol representing the mean. Differences are plotted with respect to atmospheric pressure on a logarithmic scale.

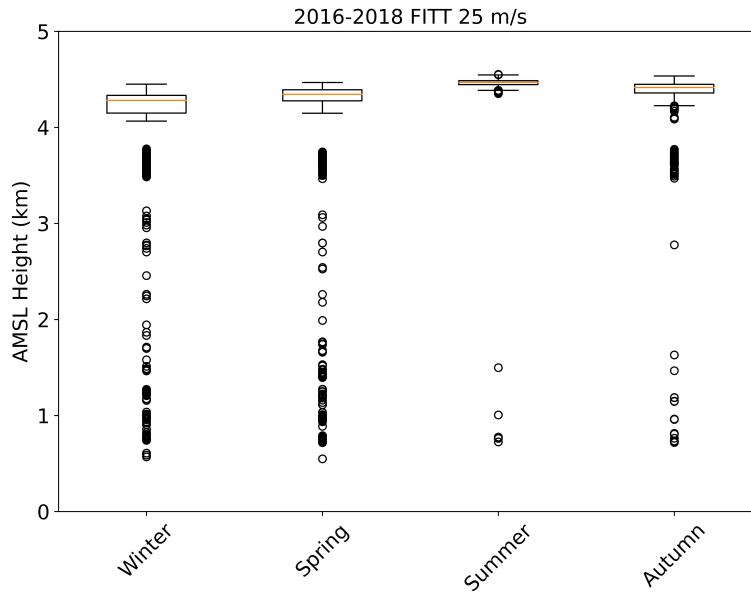


Figure 13: The maximum height reached for the FITT site given a maximum wind speed tolerance of 25 m s^{-1} .

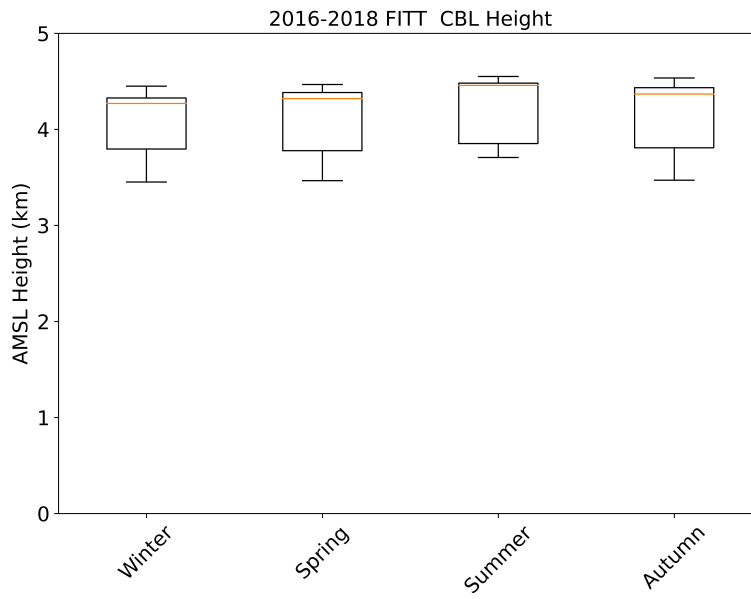


Figure 14: The maximum height reached for the FITT site given the CBL height restriction.

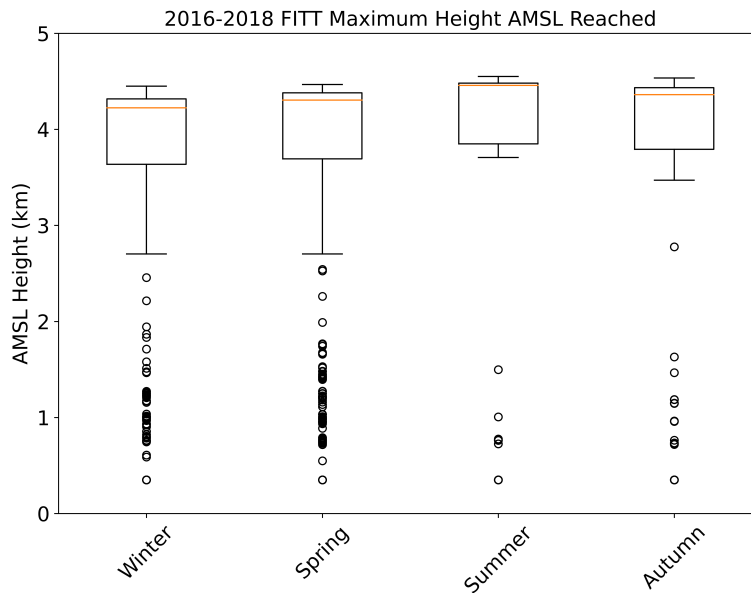


Figure 15: The maximum height reached for the FITT site.

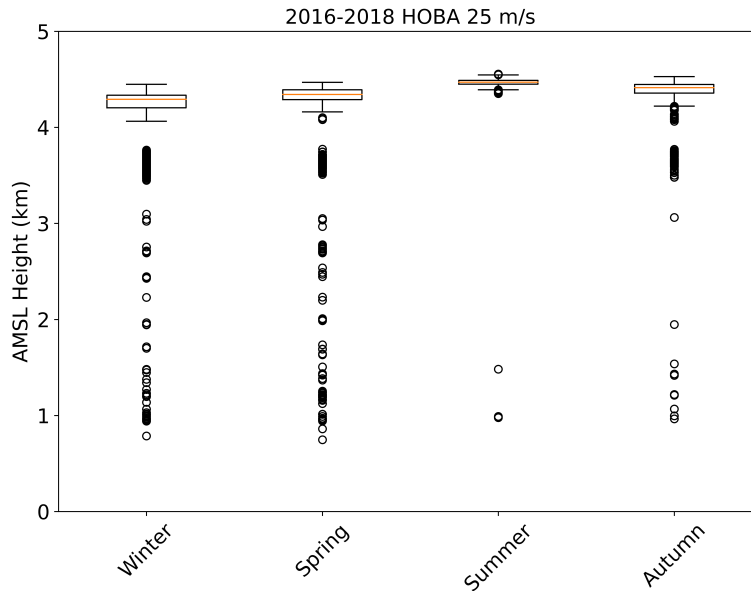


Figure 16: The maximum height reached for the HOBA site given a maximum wind speed tolerance of 25 m s^{-1} .

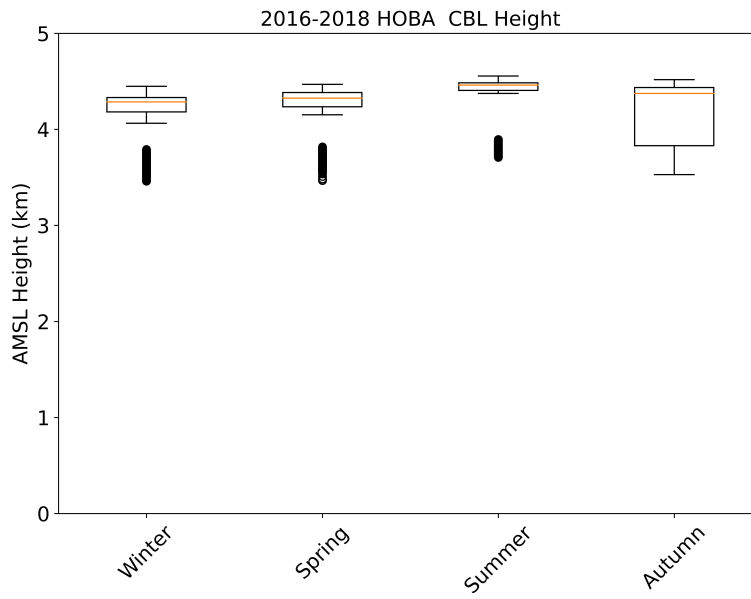


Figure 17: The maximum height reached for the HOBA site given the CBL height restriction.

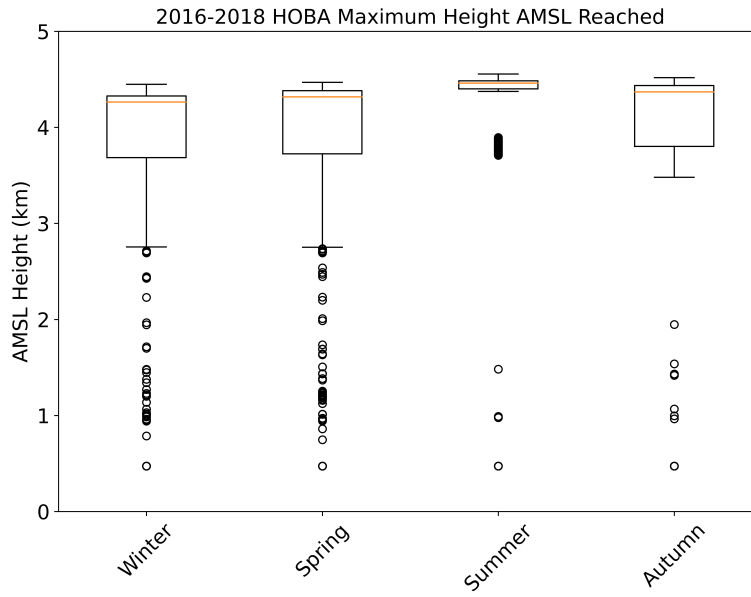


Figure 18: The maximum height reached for the HOBA site.

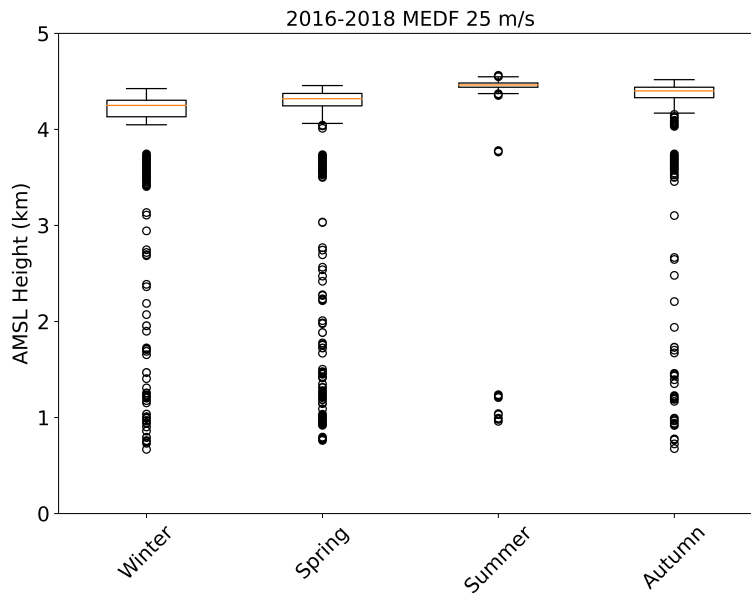


Figure 19: The maximum height reached for the MEDF site given a maximum wind speed tolerance of 25 m s^{-1} .

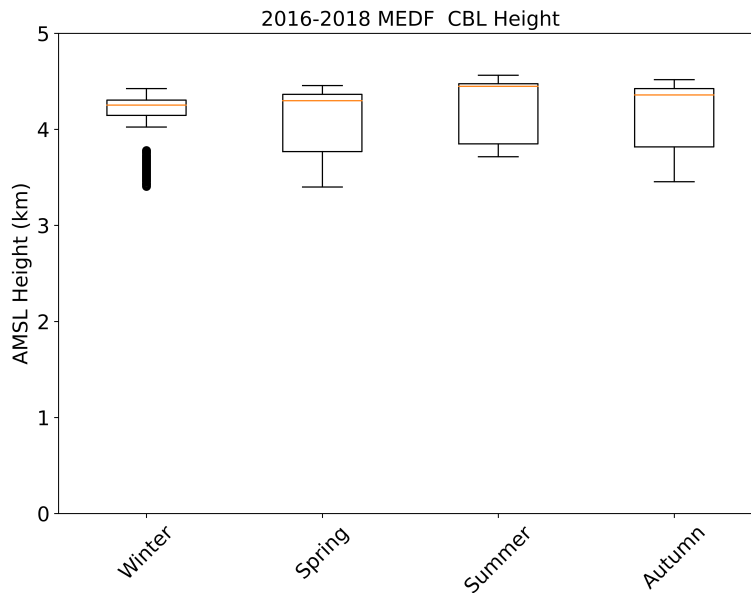


Figure 20: The maximum height reached for the MEDF site given the CBL height restriction.

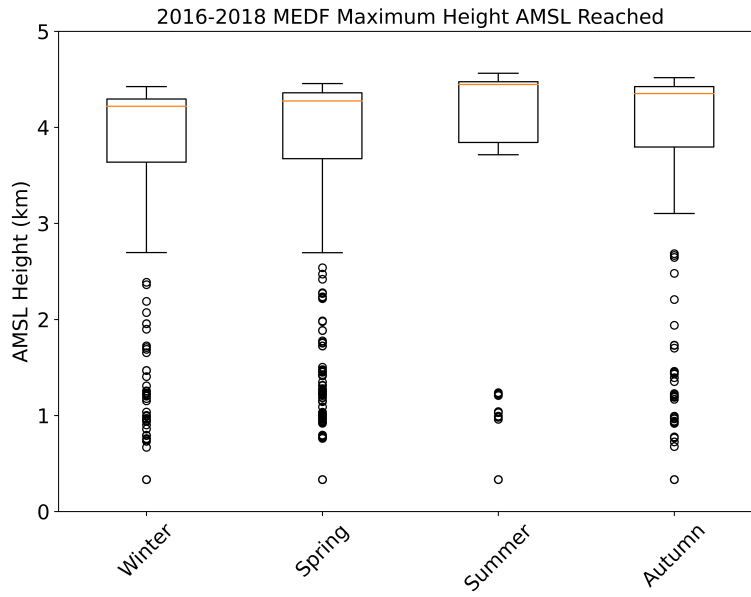


Figure 21: The maximum height reached for the MEDF site.

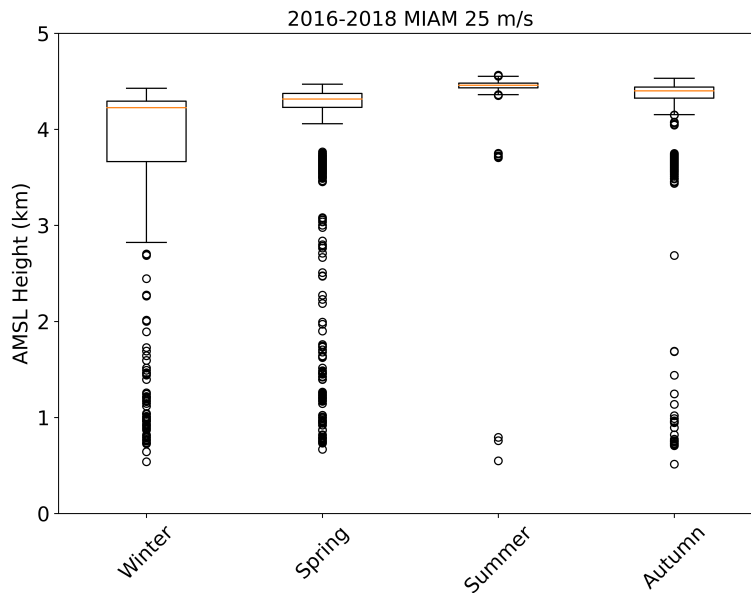


Figure 22: The maximum height reached for the MIAM site given a maximum wind speed tolerance of 25 m s^{-1} .

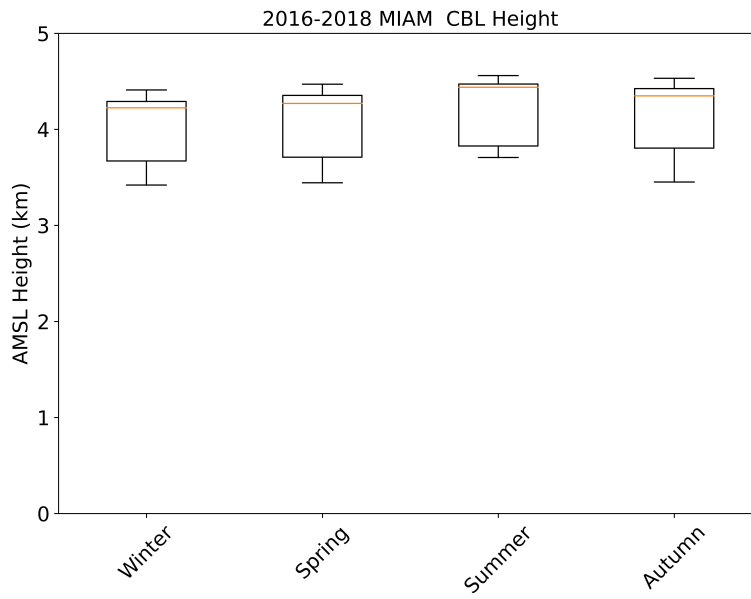


Figure 23: The maximum height reached for the MIAM site given the CBL height restriction.

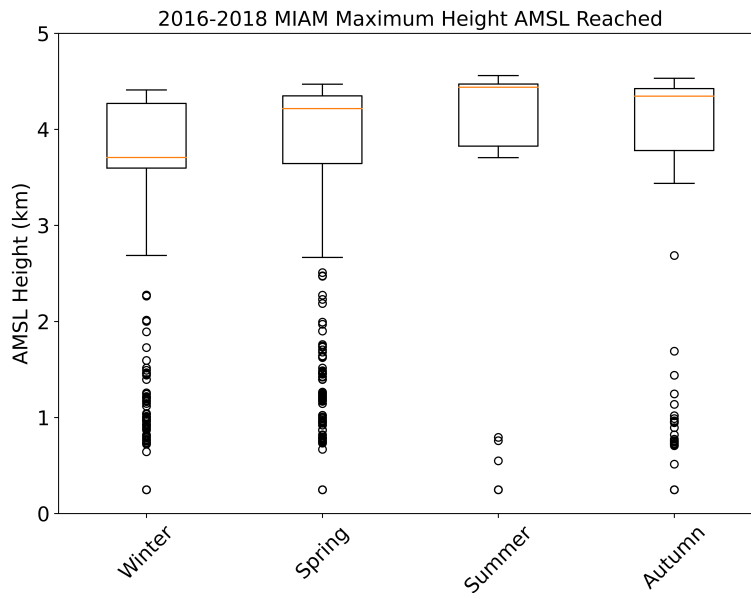


Figure 24: The maximum height reached for the MIAM site.

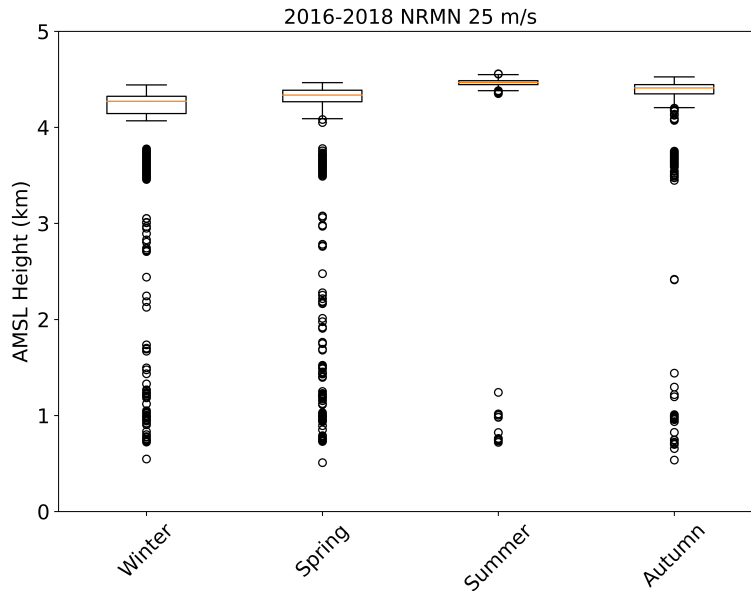


Figure 25: The maximum height reached for the NRMN site given a maximum wind speed tolerance of 25 m s^{-1} .

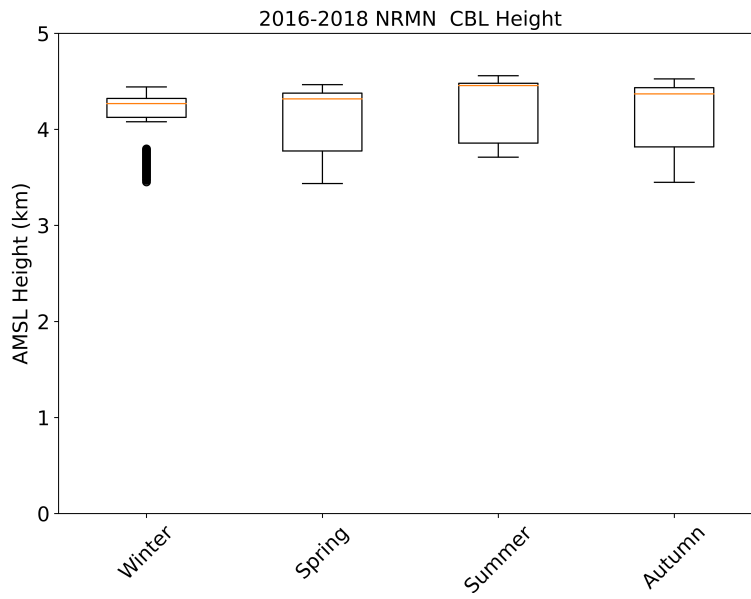


Figure 26: The maximum height reached for the NRMN site given the CBL height restriction.

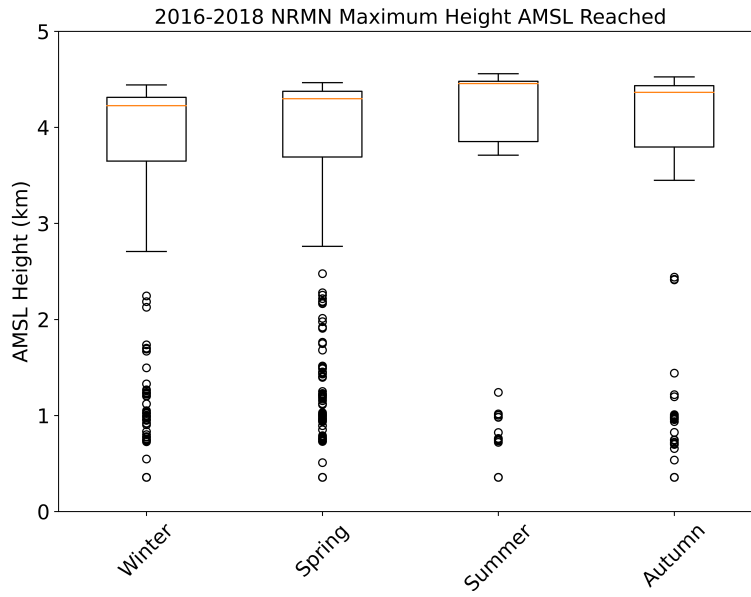


Figure 27: The maximum height reached for the NRMN site.

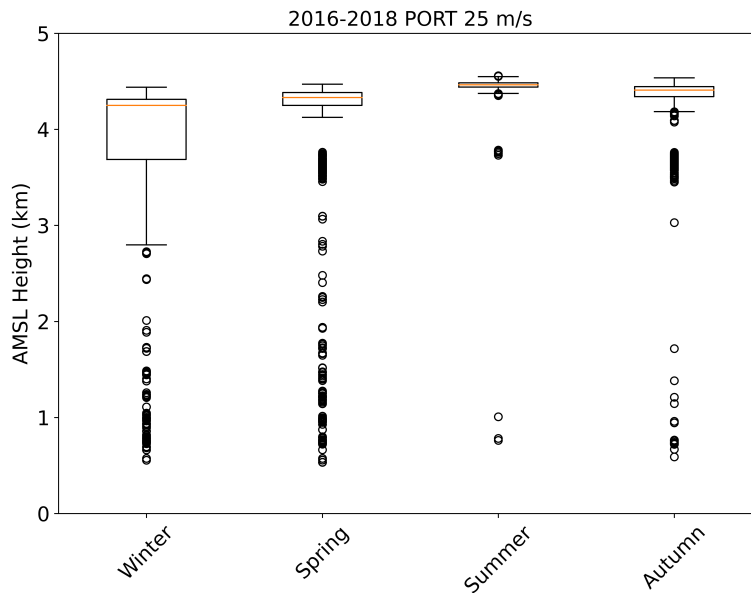


Figure 28: The maximum height reached for the PORT site given a maximum wind speed tolerance of 25 m s^{-1} .

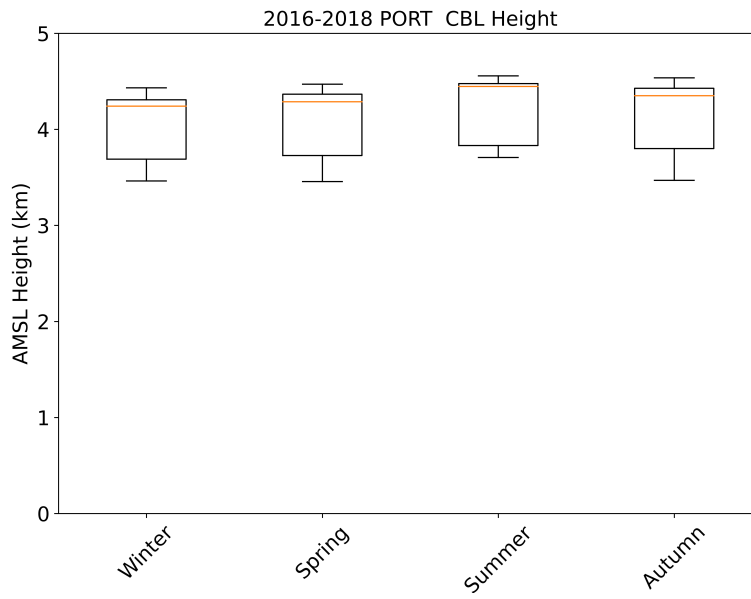


Figure 29: The maximum height reached for the PORT site given the CBL height restriction.

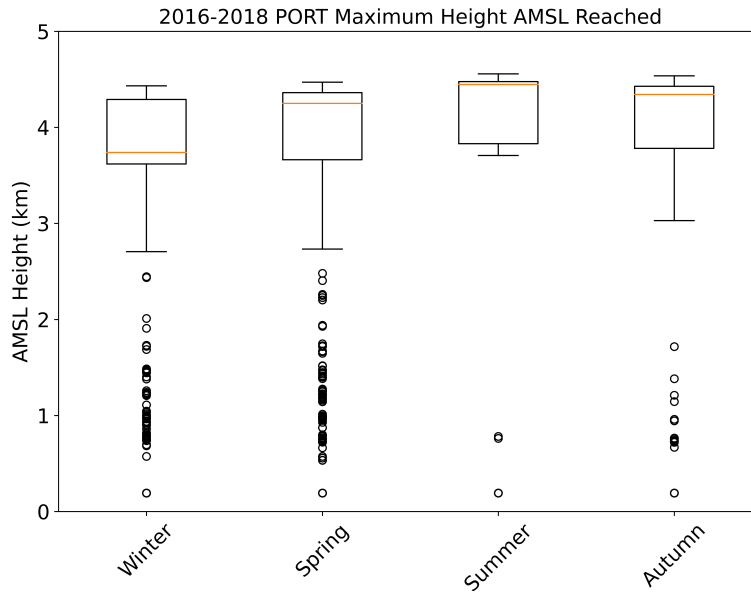


Figure 30: The maximum height reached for the PORT site.

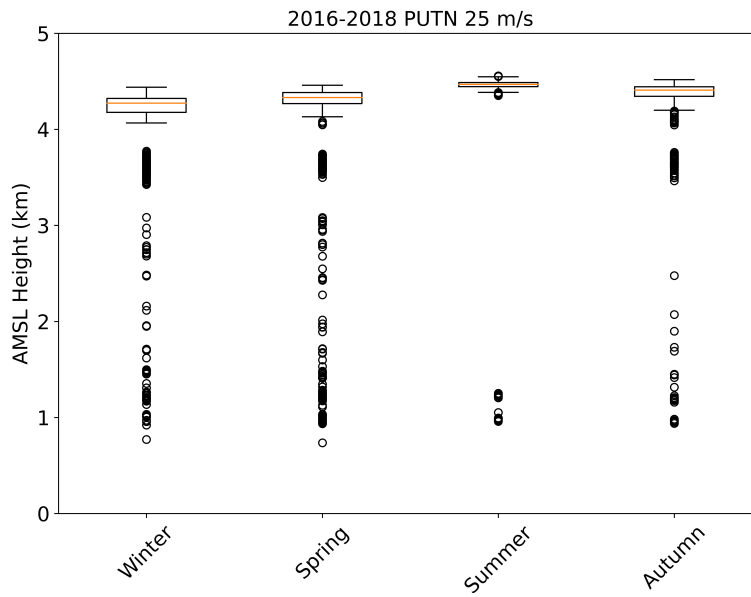


Figure 31: The maximum height reached for the PUTN site given a maximum wind speed tolerance of 25 m s^{-1} .

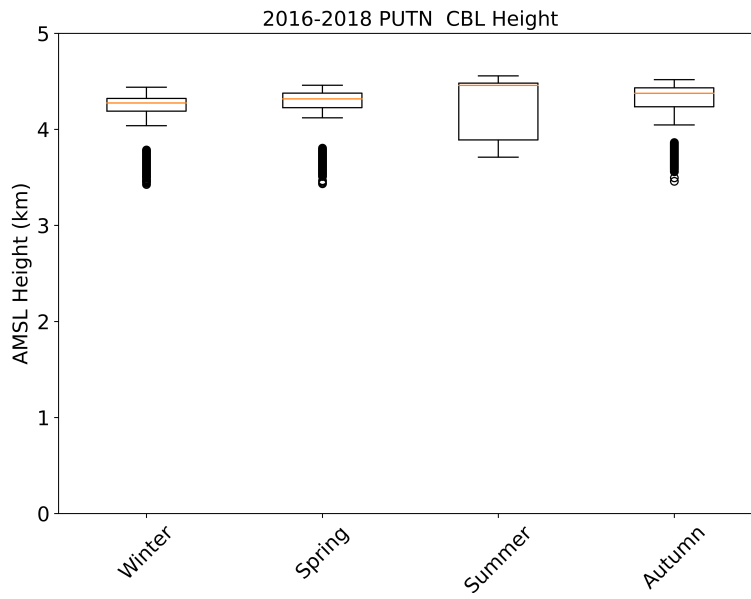


Figure 32: The maximum height reached for the PUTN site given the CBL height restriction.

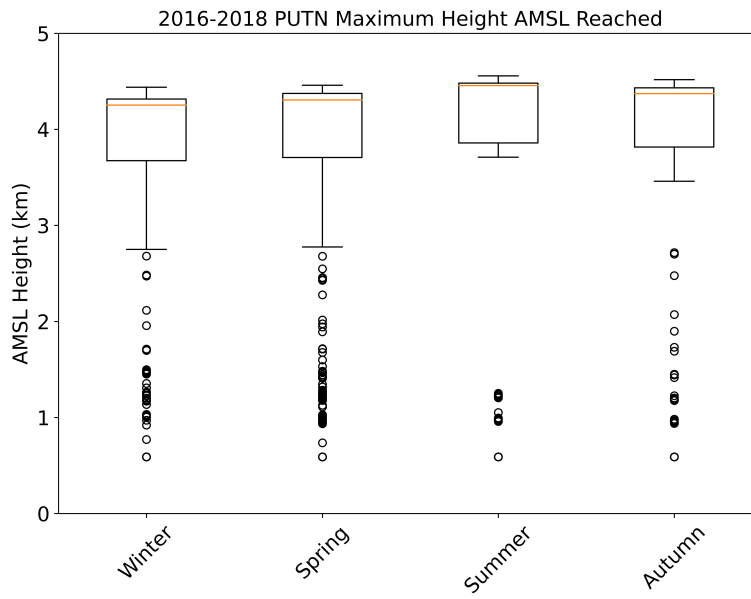


Figure 33: The maximum height reached for the PUTN site.